Nondivergent deflection of light around a photon sphere of a compact object

Ryuya Kudo and Hideki Asada
Graduate School of Science and Technology, Hirosaki University, Aomori 036-8561, Japan

(Received 6 January 2022; revised 23 February 2022; accepted 22 March 2022; published 11 April 2022)

We demonstrate that the location of a stable photon sphere (PS) in a compact object is not always an edge such as the inner boundary of a black hole shadow, whereas the location of an unstable PS is known to be the shadow edge; notably, in the Schwarzschild black hole. If a static spherically symmetric (SSS) spacetime has the stable outermost PS, the spacetime cannot be asymptotically flat. A nondivergent deflection is caused for a photon traveling around a stable PS, though a logarithmic divergent behavior is known to appear in most of SSS compact objects with an unstable photon sphere. The reason for the nondivergence is that the closest approach of a photon is prohibited in the immediate vicinity of the stable PS when the photon is emitted from a source (or reaches a receiver) distant from a lens object. The finite gap size depends on the receiver and source distances from the lens as well as the lens parameters. The mild deflection angle of light can be approximated by an arcsine function. A class of SSS solutions in Weyl gravity exemplify the nondivergent deflection near the stable outer PS.

DOI: 10.1103/PhysRevD.105.084014

I. INTRODUCTION

Since the first measurement by Eddington *et al.* [1], the gravitational deflection of light has offered us a powerful tool for tests of gravitational theories including the theory of general relativity as well as for astronomical probes of dark matter. The Event Horizon Telescope (EHT) team has recently succeeded in taking a direct image of the immediate vicinity of the central black hole candidate of M87 galaxy [2]. In addition, the same team has just reported measurements of linear polarizations around the same black hole candidate [3], which has led to an estimation of the mass accretion rate [4]. These observations have increased our renewed interest in the strong deflection of light in the strong-gravity region.

The strong deflection of light by Schwarzschild black hole was pointed out by Darwin [5]. This phenomena is closely related with a photon sphere (PS) that, with a horizon, features black holes and other compact objects [6–40]. A photon surface for a less symmetric case is a generalization of PSs [13].

Many years later, Bozza showed that the strong deflection behavior in Schwarzschild black hole can be well described as the logarithmic divergence in the deflection angle [6]. Such a strong deflection as the logarithmic divergence also occurs in other exotic objects such as wormholes. For instance, Tsukamoto conducted several extensions of the Bozza method for the strong deflection of light [7,8], in which the logarithmic behavior is shown to be a quite general feature for a static and spherically symmetric (SSS) compact object that has a PS, e.g., Ellis wormholes. The logarithmic behavior in the strong deflection for a finite-distance receiver and source has been recently confirmed [41] by solving the exact gravitational lens that stands even for an asymptotically nonflat spacetime [42–44].

There exists a single PS outside the horizon of the Schwarzschild black hole, while Ellis wormhole has a PS without horizons. For both cases, the number of PSs is one. Tsukamoto obtained the logarithmic behavior for such a SSS spacetime with a single PS, which was assumed to be unstable. In both of Schwarzschild black hole and Ellis wormhole, there exists only the unstable PS. Cunha *et al.* have recently proven that ultracompact objects have an even number of PSs, one of which is stable [45]. Regarding the proven theorem, Hod has found an exception for horizonless spacetimes that possess no stable PS [46]. What happens, if the PS is stable and a light ray is deflected around the stable PS?

The main purpose of the present paper is to study the deflection of light around a PS when the PS is stable in a SSS spacetime. This situation has not often been considered in detail e.g., [5–7,9,10], except for Hasse and Perlick (2002) [47] which provided a theorem on a connection among the three properties of (1) the presence of a PS for a saddle point case and a stable case as well as an unstable one, (2) the centrifugal force reversal, and (3) infinitely many images in any SSS spacetime. However, Hasse and Perlick (2002), did not calculate the deflection angle of light, because they focused on the multiple imaging [47]. We shall show that, instead of the logarithmic type of strong deflection, a mild deflection is caused near the stable PS.

This paper is organized as follows. In Sec. II, we reexamine the deflection angle of light when there exists

 © 2022 American Physical Society

a stable outer PS in a SSS spacetime. In Sec. III, we study how light is deflected in the presence of the stable outer PS. It is shown that the deflection behavior is not too strong to make the logarithmic divergence but mild enough to be approximated by an arcsine function. As an example for such a mild deflection of light, we consider a class of Weyl gravity model in Sec. IV. Section V concludes the present paper. Throughout this paper, we use the unit of $G = c = 1$.

II. DEFLECTION ANGLE INTEGRAL

A. SSS spacetime

We consider a SSS spacetime, for which the metric reads

$$ds^2 = -A(r)dt^2 + B(r)dr^2 + C(r)(d\theta^2 + \sin^2\theta d\phi^2), \quad (1)$$

where $A(r) > 0$, $B(r) > 0$, and $C(r) > 0$ are assumed to be finite. If the SSS spacetime possesses a horizon, we focus on the outside of the horizon. We do not assume the asymptotic flatness of the spacetime. Actually, the present paper considers an asymptotically nonflat case. A lemma on this issue is given at the end of the present section.

B. Photon orbits

Without loss of generality, we can consider a photon orbit on the equatorial plane ($\theta = \pi/2$) because of the spherical symmetry of the spacetime. On the equatorial plane in the SSS spacetime, a light ray has two constants of motion. One is the specific energy $E \equiv A(r)\dot{t}$ and the other is the specific angular momentum $L \equiv C(r)\dot{\phi}$, where the overdot denotes the derivative with respect to the affine parameter λ along the light ray.

By using the two constants E and L, the impact parameter of light becomes $b = L/E$. Without loss of generality, we assume $b > 0$.

In terms of b, the null condition $ds^2 = 0$ is rearranged as the orbit equation

$$\dot{r}^2 + V(r) = 0, \quad (2)$$

where $V(r)$ is defined as

$$V(r) \equiv -\frac{L^2 F(r)}{B(r)C(r)}. \quad (3)$$

Here,

$$F(r) \equiv \frac{C(r)}{A(r)b^2} - 1. \quad (4)$$

The closest approach of a light ray is denoted as r_0, which satisfies $V(r_0) = 0$ from the definition of r_0. Henceforth, evaluation at $r = r_0$ is indicated by the subscript 0. For instance, $V(r_0) = 0$ is equivalent to $F_0 = 0$, where $F_0 \equiv F(r_0)$. By combining $F_0 = 0$ and Eq. (4), we obtain

$$b = \sqrt{\frac{C_0}{A_0}}. \quad (5)$$

This offers a relation between b and r_0.

Following Hasse and Perlick [47], we use a particular form of the potential $\tilde{V}(r)$ that is defined as

$$\tilde{V}(r) \equiv \frac{A(r)}{C(r)}, \quad (6)$$

which is conformally invariant. Thereby, Eq. (2) is rewritten as

$$A(r)B(r)\dot{r}^2 + L^2\tilde{V}(r) - E^2 = 0. \quad (7)$$

This simplifies the analysis of the photon sphere and its linear perturbation, because $V(r)$ depends on b as well as r, whereas $\tilde{V}(r)$ does not include b. The potential $\tilde{V}(r)$ plays the central role in the proof of a theorem that clarifies a connection among three properties of the presence of a PS, the centrifugal force reversal, and infinitely many images in any SSS spacetime [47].

For later convenience, we write down the first and second derivatives of $\tilde{V}(r)$,

$$\tilde{V}'(r) = -\frac{A(r)D(r)}{C(r)}, \quad (8)$$

$$\tilde{V}''(r) = -\frac{A(r)}{C(r)}[D'(r) - D(r)^2], \quad (9)$$

where the prime denotes the differentiation with respect to r, and the functions D is defined as

$$D(r) \equiv \frac{C'(r)}{C(r)} - \frac{A'(r)}{A(r)}. \quad (10)$$

From Eq. (7), we obtain

$$[A(r)B(r)]'\dot{r}^2 + 2A(r)B(r)\dot{r}\ddot{r} + L^2\tilde{V}'(r) = 0. \quad (11)$$

Equations (7) and (11) tell us that a photon orbit is a circle if and only if $r = r_m$ satisfies $\tilde{V}(r_m) = (b_m)^{-2}$ and $\tilde{V}'(r_m) = 0$, where r_m denotes the radius of the PS and the subscript m denotes the value at $r = r_m$. From $\tilde{V}(r_m) = (b_m)^{-2}$, the impact parameter for the PS is obtained as

$$b_m = \sqrt{\frac{C_m}{A_m}}, \quad (12)$$

where Eq. (6) is used.

C. Classification of PS stability

We consider a small displacement δr around the PS orbit, $r = r_m + \delta r$. At the linear order in δr, Eq. (11) gives

$$\frac{d^2}{d\lambda^2}(\delta r) = -\frac{L^2\tilde{V}''(r_m)}{2A_mB_m}\delta r = \frac{L^2D_m'}{2B_mC_m}\delta r, \tag{13}$$

where Eq. (9) and $D(r_m) = 0$ from $\tilde{V}'(r_m) = 0$ are used.

The linear stability of the perturbed orbit is determined only by the sign of D_m', because $A(r) > 0$, $B(r) > 0$, $C(r) > 0$, and $L \neq 0$. A PS is stable if $D_m' < 0$, whereas it is unstable for $D_m' > 0$.

From Eq. (10), we obtain

$$D'(r) = \frac{C''(r)}{C(r)} - \frac{A''(r)}{A(r)} - D(r)\left(\frac{C'(r)}{C(r)} + \frac{A'(r)}{A(r)}\right). \tag{14}$$

On the PS, this is reduced to

$$D_m' = \frac{C_m''}{C_m} - \frac{A_m''}{A_m}. \tag{15}$$

Bozza and Tsukamoto assumed $D_m' > 0$, which means an unstable PS [6,7]. Henceforth, we focus on a stable case $D_m' < 0$. Such an unusual case is realized in a class of Weyl gravity model as shown in Sec. VI.

D. Total angle integral

From Eq. (2), we obtain

$$\frac{dr}{d\phi} = \pm\sqrt{\frac{C(r)F(r)}{B(r)}}, \tag{16}$$

for which we choose the plus sign without loss of generality. Integrating this from a source (denoted as S) to a receiver (denoted as R) leads to the total change in the longitudinal angle.

$$I_F(r_S, r_R, r_0) \equiv \sum_{i=S,R}\int_{r_0}^{r_i}\frac{dr}{\sqrt{\frac{C(r)F(r)}{B(r)}}}. \tag{17}$$

Note that a conventional method discusses the total integral I for the asymptotic receiver and source ($r_R \to \infty$ and $r_S \to \infty$) e.g., [5–7], for which $I - \pi$ gives the deflection angle of light. On the other hand, the present paper considers finite distance between the receiver and source. In order to clarify this difference, we use I_F in stead of I. Rigorously speaking, $I_F - \pi$ is not the deflection angle but I_F is the dominant component of the deflection angle. This issue is beyond the scope of this paper. See e.g., Refs. [48–51] on how to define geometrically the deflection angle for the finite-distance receiver and source.

Following Bozza and Tsukamoto [6,7], we introduce a variable as

$$z \equiv 1 - \frac{r_0}{r}, \tag{18}$$

to rewrite Eq. (17) as

$$I_F(z_S, z_R, r_0) = \sum_{i=S,R}\int_0^{z_i} f(z, r_0)dz, \tag{19}$$

where we define $z_i \equiv 1 - r_0/r_i$ $(i = R, S)$,

$$H(z, r_0) \equiv \frac{CF}{B}(1-z)^4, \tag{20}$$

and

$$f(z, r_0) \equiv \frac{r_0}{\sqrt{H(z, r_0)}}. \tag{21}$$

In the next subsection we shall examine the integrand in Eq. (19).

E. Analysis in the vicinity of PS

By noting $F_0 = 0$, the function H is expanded around $r = r_0$ $(z = 0)$ as

$$H(z, r_0) = \sum_{n=1}^{\infty} c_n(r_0)z^n, \tag{22}$$

where

$$c_1(r_0) = \frac{C_0D_0r_0}{B_0}, \tag{23}$$

$$c_2(r_0) = \frac{C_0}{B_0}\left[D_0r_0\left(\frac{C_0'}{C_0} - \frac{B_0'}{B_0} - 3\right) + \frac{r_0^2}{2}(D_0^2 + D_0')\right], \tag{24}$$

$$c_3(r_0) = \frac{C_0}{B_0}\left[D_0r_0\left(\frac{3B_0'r_0}{B_0} - \frac{3C_0'r_0}{C_0} - \frac{B_0'C_0'r_0^2}{B_0C_0} - 3\right) + \frac{r_0^2}{2}(D_0^2 + D_0')\left(\frac{C_0'r_0}{C_0} - \frac{B_0'r_0}{B_0} - 2\right) + \frac{r_0^3}{6}(D_0^3 + 3D_0'D_0 + D_0'')\right]. \tag{25}$$

When the closest approach is located near the PS ($r_0 = r_m$), Eqs. (23)–(25) become

$$c_1(r_m) = 0, \tag{26}$$

$$c_2(r_m) = \frac{r_m^2C_mD_m'}{2B_m}, \tag{27}$$

$$c_3(r_m)=\frac{r_m^2 C_m}{2B_m}\left[D'_m\left(\frac{C'_m r_m}{C_m}-\frac{B'_m r_m}{B_m}-2\right)+\frac{r_m D''_m}{3}\right]. \quad (28)$$

From Eqs. (26)–(28), we find

$$H(z,r_m)=c_2(r_m)z^2+O(z^3). \quad (29)$$

If the PS is unstable (stable), namely $D'_m>0$ ($D'_m<0$), then, $c_2(r_m)>0$ (<0). As pointed by Tsukamoto [7], the angle integral I_F by Eq. (17) is divergent logarithmically. On the other hand, the stable PS case ($c_2(r_m)<0$) is investigated below in detail.

Before closing this section, we mention a relation of the emergence of the stable outermost PS (SOPS) and the spacetime asymptotic flatness.

Lemma: If a SSS spacetime has the SOPS, the spacetime cannot be asymptotically flat, for which $\tilde{V}'(r)=[A(r)/C(r)]'$ is positive everywhere outside the SOPS.

Proof: We denote the radius of the SOPS as $r_{\rm SOPS}$. At the location of the SOPS, $\tilde{V}'(r_{\rm SOPS})=0$ and $\tilde{V}''(r_{\rm SOPS})>0$. There exist no PSs outside of the SOPS, because the SOPS is the outermost PS. Therefore, $\tilde{V}''(r)>0$ for $r>r_{\rm SOPS}$. This means that $\tilde{V}'(r)$ is an *increasing* function of r when $r>r_{\rm SOPS}$. Hence, $\tilde{V}'(r)>0$ for $r>r_{\rm SOPS}$.

Here, we add an assumption that the spacetime were asymptotically flat. Then, we can employ a coordinate system in which Eq. (1) approaches the Minkowski metric in the polar coordinates asymptotically as $r\to\infty$. Namely, $A(r)\to 1+O(1/r)$ and $C(r)\to r^2+O(r)$, which lead to $A'(r)\to O(1/r^2)$ and $C'(r)\to 2r+O(r^0)$. Thereby,

$$\tilde{V}'(r)=\left(\frac{A(r)}{C(r)}\right)'=-\frac{2}{r^3}+O\left(\frac{1}{r^4}\right)\to 0, \quad (30)$$

in the limit as $r\to\infty$. This means that $\tilde{V}'(r)$ has an extremum between $r_{\rm SOPS}$ and $r=\infty$, because of its continuity. This contradicts with that $\tilde{V}'(r)$ is an increasing function for $r>r_{\rm SOPS}$. Therefore, the spacetime is not asymptotically flat. A proof of the lemma is thus completed.

According to Ref. [35], if an axisymmetric, stationary and asymptotically flat spacetime possesses light rings (LRs), the outest LR is unstable. This means that if a SSS spacetime with PSs is asymptotically flat, the outermost PS is unstable. The contraposition of this is that, if the outermost PS in a SSS spacetime with PSs is stable, the spacetime is not asymptotically flat. This proves a part of the above lemma but tells us nothing about the positivity of $\tilde{V}'(r)$ for $r>r_{\rm SOPS}$.

On the other hand, it is clear that the asymptotic flatness is allowed, if the outermost PS (OPS) is unstable [$\tilde{V}''(r_{\rm OPS})<0$]. In the rest of this paper we consider that a receiver and source are located outside of a stable outer PS. However, it is not specified below whether or not it is the outermost.

Before closing the section, let us briefly mention the stability of a spacetime that admits a stable PS. Horizonless ultracompact objects with a stable PS may suffer from instabilities due to slowly (at most logarithmically) decaying of perturbations leading to the formation of a trapped surface [45,52–54]. In Sec. VI, therefore, we consider a black hole model with a stable PS in Weyl gravity. On the other hand, the above lemma may suggest another possibility compatible with the instability arguments in Refs. [45,52–54]. One such candidate is a compact object without a black hole horizon but with a stable PS and a cosmological horizon that is consistent with the asymptotic nonflatness. Its stability issue is beyond the scope of the present paper.

III. MILD DEFLECTION NEAR THE STABLE OUTER PS

A. Stability classification of the outer PS

In the neighborhood of the closest approach $z\sim 0$, higher order terms of $H(z,r_m)$ in Eq. (22) are negligible compared with z and z^2 terms. The dominant part of $f(z,r_0)$ for $r_0\sim r_m$ thus becomes

$$f_D(z,r_0)\equiv\frac{r_0}{\sqrt{h(z)}}, \quad (31)$$

where $h(z)$ is defined as

$$h(z)=c_1(r_0)z+c_2(r_0)z^2. \quad (32)$$

Associated with $f_D(z,r_0)$, we define the dominant part of the total angle integral as

$$I_{\rm FD}(z_R,z_S,r_0)\equiv\sum_{i=S,R}\int_0^{z_i} f_D(z,r_0)dz. \quad (33)$$

Before starting calculations of the angle integral, first we investigate a photon orbit in the stable PS case. If $c_1(r_0)<0$, $h(z)$ is always negative for $z>0$. This is in contradiction with the non-negativity of $h(z)$. Hence, the case of $c_1(r_0)<0$ is discarded. If $c_1(r_0)=0$, then, $h(z)=c_2(r_0)z^2$. The non-negativity of $h(z)$ together with $c_2(r_0)<0$ admits only $z=0$. This orbit is a circle. We do not discuss this special case any more. For the last case $c_1(r_0)>0$, the non-negativity of $h(z)$ provides a nontrivial situation; the allowed region for z is

$$0\le z\le -\frac{c_1(r_0)}{c_2(r_0)}. \quad (34)$$

This means that only bound orbits are allowed, whereas the scattering orbits are prohibited. Note that $h(z)=0$ does not make the integral in Eq. (33) divergent. Indeed, $h(z)\sim c_1(r_0)z$ near a point $z=0$ and $h(z)\sim -c_1(r_0)[z+c_1(r_0)/c_2(r_0)]$ near a point $z\sim -c_1(r_0)/c_2(r_0)$. At the two points, therefore,

the integral of $h(z)$ is not divergent as $\sim \int z^{-1/2} dz \sim 2\sqrt{z}$. The two points $z = 0$ and $z \sim -c_1(r_0)/c_2(r_0)$ are the periastron and apastron, respectively.

B. Angle integral for the stable outer PS

Henceforth, we focus on the case of $c_1(r_0) > 0$, for which the receiver and source positions satisfy

$$0 < z_i \leq -\frac{c_1(r_0)}{c_2(r_0)}. \tag{35}$$

Equation (33) is integrated as

$$I_{\rm FD}(z_R, z_S, r_0) = \frac{r_0}{\sqrt{-c_2(r_0)}} \times \left[\pi - \sum_{i=S,R} \arcsin\left(1 + \frac{2c_2(r_0)}{c_1(r_0)} z_i\right)\right]. \tag{36}$$

It follows that the arcsine term in Eq. (36) is well defined for the allowed region by Eq. (35), because

$$-1 \leq 1 + \frac{2c_2(r_0)}{c_1(r_0)} z_i < 1. \tag{37}$$

C. I_F in terms of b

In most of lens studies including Refs. [6,7], it is convenient to express the deflection angle in terms of the impact parameter in stead to r_0, mainly because $b \sim D_L\theta$ for the lens distance D_L and the image angle direction θ.

Therefore, we look for an approximate expression of b. Near the PS, $c_1(r_0)$ and $b(r_0)$ are Taylor expanded as

$$c_1(r_0) = \frac{C_m r_m D'_m}{B_m}(r_0 - r_m) + O((r_0 - r_m)^2), \tag{38}$$

$$b(r_0) = b_m + \frac{b_m D'_m}{4}(r_0 - r_m)^2 + O((r_0 - r_m)^3). \tag{39}$$

From Eq. (38), we find

$$r_0 < r_m, \tag{40}$$

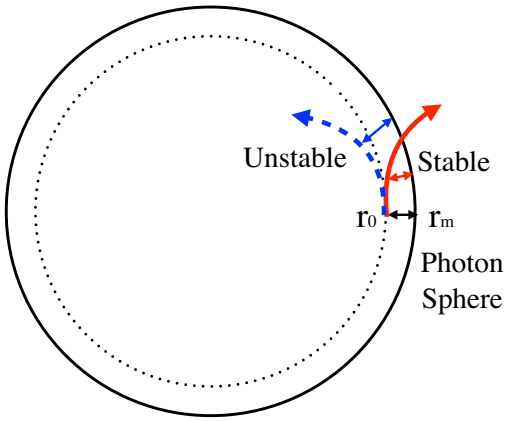

FIG. 1. Schematic figure of photon orbits near a PS. The PS is denoted by a solid circle with radius r_m. The dotted circle has radius r_0, which is slightly smaller than r_m. Namely, $r_m - r_0$ is taken as a perturbation around the PS. The initial position of the photon is r_0, at which the initial radial velocity is vanishing. The thick dashed blue (in color) arrow denotes a photon motion when the PS is unstable. The orbital deviation grows because of being unstable. Therefore, it is difficult for the inner photon to escape to a far region. This is why the earlier papers focused on $r_0 > r_m$ when an unstable PS is assumed [6,7]. On the other hand, the thick solid red (in color) arrow denotes a photon motion when the PS is stable. The orbital deviation gets smaller because of being stable. It is thus possible that the inner photon ($r_0 < r_m$) crosses the PS to reach a distant observer.

where $c_1(r_0) > 0$ and $D'_m < 0$ are used. This inequality means that the light ray passes by the slight inside of the PS. This is because the PS is stable. This unusual behavior of the photon orbit implies also

$$b < b_m, \tag{41}$$

from Eq. (39). See Fig. 1 for the photon orbit behavior near the PS.

By combining Eqs. (38) and (39), we obtain, near the PS, an approximate relation between $c_1(r_0)$ and b as

$$c_1(r_0) \approx \frac{2r_m C_m \sqrt{-D'_m}}{B_m}\left(1 - \frac{b}{b_m}\right)^{\frac{1}{2}}. \tag{42}$$

By substituting this into Eq. (36), we obtain

$$I_{\rm FD}(z_R, z_S, b) \simeq \frac{r_m}{\sqrt{-c_2(r_m)}}\left[\pi - \sum_{i=S,R} \arcsin\left\{1 - \frac{r_m\sqrt{-D'_m}}{2}\left(1 - \frac{b}{b_m}\right)^{-\frac{1}{2}} z_i\right\}\right]. \tag{43}$$

By direct calculations for a photon traveling near the PS, Eq. (35) is rearranged as

$$0 < z_i \leq \frac{4}{r_m\sqrt{-D'_m}}\left(1 - \frac{b}{b_m}\right)^{1/2}, \tag{44}$$

for which the arcsine function in Eq. (43) is well defined.

In order to obtain Eq. (43) as an approximate estimation of I_F in terms of b, we have used the Taylor series expansion as Eq. (39), which is valid if $b_m > b_m|D'_m|(r_0 - r_m)^2/4$. This requires that the closest approach of light and the PS are close enough to satisfy

$$|r_0 - r_m| < \frac{2}{\sqrt{|D'_m|}}. \tag{45}$$

Yet, a lower bound on $|r_0 - r_m|$ exists in the neighborhood of the PS as shown below.

D. Discontinuity between the closest approach and the stable PS

Equation (44) suggests a proposition on the existence of a gap between the allowed closest approach and the stable PS.

Proposition: In a SSS spacetime which possesses a stable outer photon sphere, the closest approach of a photon from a source (or to a receiver) located at a finite distance from the lens object is not allowed in the infinitesimal neighborhood of the stable PS.

Proof: This proposition can be proven by contradiction as follows. We consider a receiver (or a source) at finite distance from the lens, namely $r_i > r_0$, which leads to $z_i > 0$. We assume the closest approach of a photon orbit were in the infinitesimal neighborhood of the stable PS.

On the stable PS, $F_m = F'_m = 0$, while $F''_m < 0$. The last inequality comes from the unstable condition $D'_m < 0$. The function F near the PS is thus Taylor expanded as

$$F_0 = \frac{1}{2}F''_m(r_0 - r_m)^2 + O((r_0 - r_m)^3). \tag{46}$$

From Eq. (20), H for $r_0 \approx r_m$ is expanded as

$$H = \frac{C_m F''_m}{2B_m}(1 - z)^4(r_0 - r_m)^2 + O((r_0 - r_m)^3), \tag{47}$$

where Eq. (46) is used.

By using $B_m > 0$, $C_m > 0$, and $F''_m < 0$ for Eq. (47), we find $H < 0$ if $r_0 - r_m$ is sufficiently small. $H < 0$ contradicts with the existence of the photon orbit. Our proof is finished.

The above proposition prohibits the closest approach in the infinitesimal neighborhood of the stable PS. However, it does not tell about a size of the gap between the allowed closest approach and the stable PS. In order to discuss the gap size, we use Eq. (44), which is rewritten as

$$\frac{b}{b_m} \le 1 - \frac{r_m^2 z_i^2(-D'_m)}{16}. \tag{48}$$

Note that Eq. (44) is based on a quadratic approximation up to z^2.

For finite z_i and $D'_m < 0$, Eq. (48) demonstrates that b is not allowed in the infinitesimal neighborhood of b_m. From Eq. (48), the upper bound on b is

$$b_{\max} = b_m - \frac{b_m r_m^2 z_L^2(-D'_m)}{16}. \tag{49}$$

The gap size $\Delta b \equiv b_m - b_{\max}$ is thus given by

$$\Delta b = \frac{b_m r_m^2 z_L^2(-D'_m)}{16}, \tag{50}$$

where z_L is the larger one of z_R and z_S, namely the value of z for the more distant one of the receiver and source.

A separate treatment is needed for the marginal PSs ($D'_m = 0$) e.g., Ref. [8,55].

E. THE DOMINANT PART AND THE REMAINDER

Before closing this section we shall confirm that $I_{FR} \equiv I_F - I_{FD}$ is really the remainder. It is written simply as

$$I_{FR}(z_R, z_S, r_0) \equiv \sum_{i=R,S} \int_0^{z_i} f_R(z, r_0) dz, \tag{51}$$

where $f_R(z, r_0) \equiv f(z, r_0) - f_D(z, r_0)$.

From Eq. (51), we obtain, for $z_i < 1$,

$$I_{FR}(z_R, z_S, r_0) = \sum_{i=R,S} [f_R(z_i, r_0) z_i + O(z_i^2)]. \tag{52}$$

For $r_0 \sim r_m$, $f(z, r_m) \sim f_D(z, r_m)$ when $z < 1$. Hence, by using the Taylor-expansion method, one may think that $f_R(z, r_m) = f(z, r_m) - f_D(z, r_m) = O(z)$. However, let us more carefully examine an asymptotic expansion of $f_R(z, r_0)$ for $z < 1$ [56]. By straightforward calculations, the asymptotic expansion of $f(z, r_0)$ for small z is obtained as

$$f(z, r_0) = \frac{r_0}{\sqrt{z c_1(r_0)}} - \frac{r_0 c_2(r_0)}{2 c_1(r_0)^{3/2}}\sqrt{z} + O(z^{3/2}). \tag{53}$$

Similarly, the asymptotic expansion of $f_D(z, r_0)$ is

$$f_D(z, r_0) = \frac{r_0}{\sqrt{z c_1(r_0)}} - \frac{r_0 c_2(r_0)}{2 c_1(r_0)^{3/2}}\sqrt{z} + O(z^{3/2}). \tag{54}$$

By bringing together Eqs. (53) and (54), we find

$$f_R(z, r_0) = O(z^{3/2}). \tag{55}$$

By using this for Eq. (52), we find

$$I_{FR}(z_R, z_S, r_0) = O(z_R^{5/2}, z_S^{5/2}). \tag{56}$$

On the other hand, Eq. (36) is expanded, for small z_R and z_S, as

$$I_{FD}(z_R, z_S, r_0) = \frac{2r_0}{\sqrt{c_1(r_0)}}(\sqrt{z_R} + \sqrt{z_S}) + O(z_R, z_S), \quad (57)$$

where $\arcsin(1-\varepsilon) = \pi/2 - \sqrt{2\varepsilon} + O(\varepsilon)$ is used.

For $z_R, z_S \ll 1$, Eqs. (56) and (57) lead to $I_{FR}(z_R, z_S, r_0) \ll I_{FD}(z_R, z_S, r_0)$. Therefore, we can safely say that I_{FD} is the dominant part and I_{FR} is the remainder.

IV. EXAMPLE: A CLASS OF WEYL GRAVITY MODEL

In the Weyl gravity model, Mannheim and Kazanas found a class of SSS solutions [57]. The metric reads

$$ds^2 = -g(r)dt^2 + g(r)^{-1}dr^2 + r^2(d\theta^2 + \sin^2\theta d\phi^2), \quad (58)$$

where

$$g(r) = 1 - 3\beta\gamma - \frac{\beta(2-3\beta\gamma)}{r} + \gamma r - \kappa r^2, \quad (59)$$

and we consider $g(r) > 0$, namely the outside of the horizon.

The allowed region for the existence of the stable outer PS is [58]

$$\beta > 0, \quad (60)$$

$$\gamma < 0, \quad (61)$$

$$\kappa < 0. \quad (62)$$

In this section, we focus on this parameter region.

We solve $D(r) = 0$ to find two roots as $r = 3\beta$ and $r = 3\beta - 2/\gamma$. They are corresponding to PSs. One is a stable PS and the other is an unstable one.

In the present case of $\gamma < 0$, the stable outer PS is located at

$$r_m = 3\beta - \frac{2}{\gamma}, \quad (63)$$

because

$$D'_m = -\frac{2}{r_m^2 g(r_m)} = -\frac{2b_m^2}{r_m^4} < 0. \quad (64)$$

The other root $r = 3\beta$ is the radius of the unstable inner PS.

Note that r_m is larger than 3β because of $\gamma < 0$. See Fig. 2 for the effective potential $V(r)$ in the Weyl gravity model with the stable outer PS.

There is a constraint on κ as [59]

$$\kappa < -\frac{\gamma^2(1-\beta\gamma)}{(2-3\beta\gamma)^2}. \quad (65)$$

Here, b_m denotes the critical impact parameter corresponding to the stable PS. It is obtained as

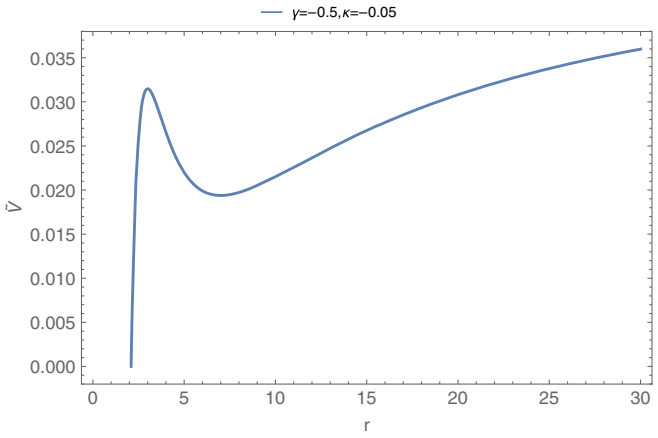

FIG. 2. Effective potential $\tilde{V}(r)$ in the Weyl gravity model. The solid blue (in color) curve corresponds to $\gamma = -0.5$ and $\kappa = -0.05$ in the unit of $\beta = 1$, which leads to the SOPS at $r_m = 7$. From $(b_m)^{-2} = \tilde{V}(r_m) = 0.0193878$, $b_m = 7.18184$ is obtained. $\tilde{V}(r)$ does not vanish for large r, because the spacetime is not asymptotically flat.

$$b_m = \frac{2-3\beta\gamma}{\sqrt{-\kappa(2-3\beta\gamma)^2 - \gamma^2(1-\beta\gamma)}}, \quad (66)$$

where the inside of the square root is always positive when κ satisfies Eq. (65).

From Eqs. (43) and (56), we obtain

$$I_{FD}(z_S, z_R, b) \simeq \pi - \sum_{i=S,R} \arcsin\left\{1 - \frac{b_m}{\sqrt{2}r_m}\left(1 - \frac{b}{b_m}\right)^{-1/2} z_i\right\}, \quad (67)$$

$$I_{FR}(z_S, z_R, b) \simeq -\beta\gamma\left(\frac{b_m}{2\sqrt{2}r_m}\right)^{3/2}\left(1 - \frac{b}{b_m}\right)^{-3/4}\sum_{i=S,R} z_i^{5/2}, \quad (68)$$

where straightforward calculations at $O(z^{5/2})$ are done in Eq. (56).

When $z_T \equiv z_R = z_S \ll (1 - b/b_m)^{1/2}$, Eq. (67) provides an approximate expression of the deflection angle as

$$\Delta\phi = I_F = 2\sqrt{\frac{\sqrt{2}b_m}{r_m}\left(1 - \frac{b}{b_m}\right)^{-1/2} z_T} + O\left(\frac{b_m}{r_m}\left(1 - \frac{b}{b_m}\right)^{-1/2} z_T\right). \quad (69)$$

where we use $\arcsin(1-\varepsilon) = \pi/2 - \sqrt{2\varepsilon} + O(\varepsilon)$ for $\varepsilon < 1$.

It is natural that I_{FR} is much smaller than I_{FD}, as discussed in Sec. III. Equation (67) shows the mild deflection in terms of the arcsine function. Figure 3 shows f. See Fig. 4 for a comparison of Eq. (67) and numerical

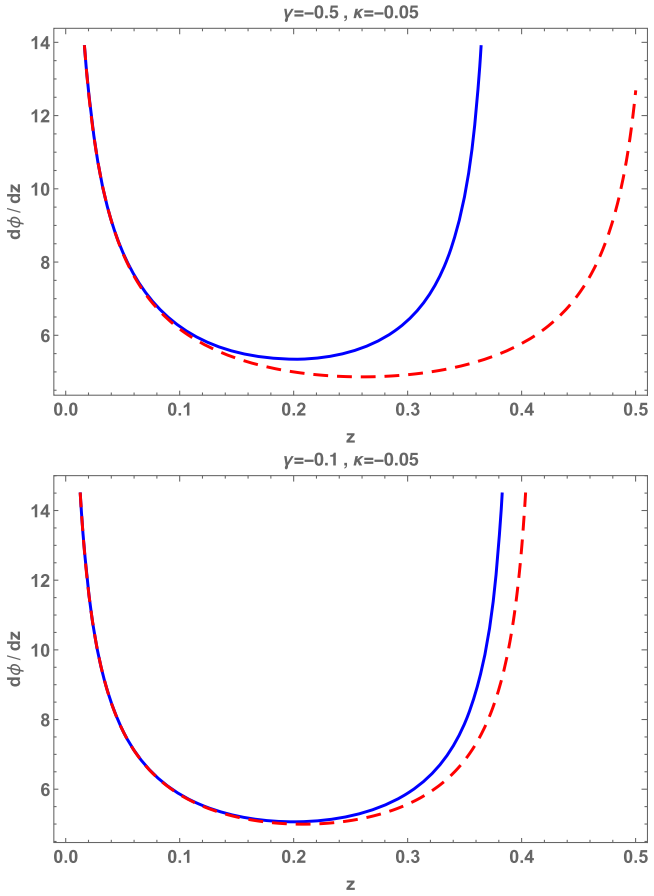

FIG. 3. The integrands of Eqs. (19) and (33). The solid blue (in color) curve denotes f $(= d\phi/dz)$ in the integral I_F, while the dashed red (in color) curve denotes f_D in I_{FD}. The horizontal axis means z. We assume $\kappa = -0.05$ in the unit of $\beta = 1$ that is roughly corresponding to the conventional unit as mass $= 1$ in the Schwarzschild or Kottler spacetime. The top and bottom panels assume $\gamma = -0.5$ and $\gamma = -0.1$, respectively, each of which leads to $r_m = 7.0$ and $b_m = 7.18185$, and $r_m = 23$ and $b_m = 4.56815$, respectively. In both cases, the solid and dashed curves are overlapped better for smaller z. For instance, the difference between them is about 10% at $z \sim 0.2$. A significant deviation at large z is due to a departure from the quadratic approximation of $H(z)$ in z.

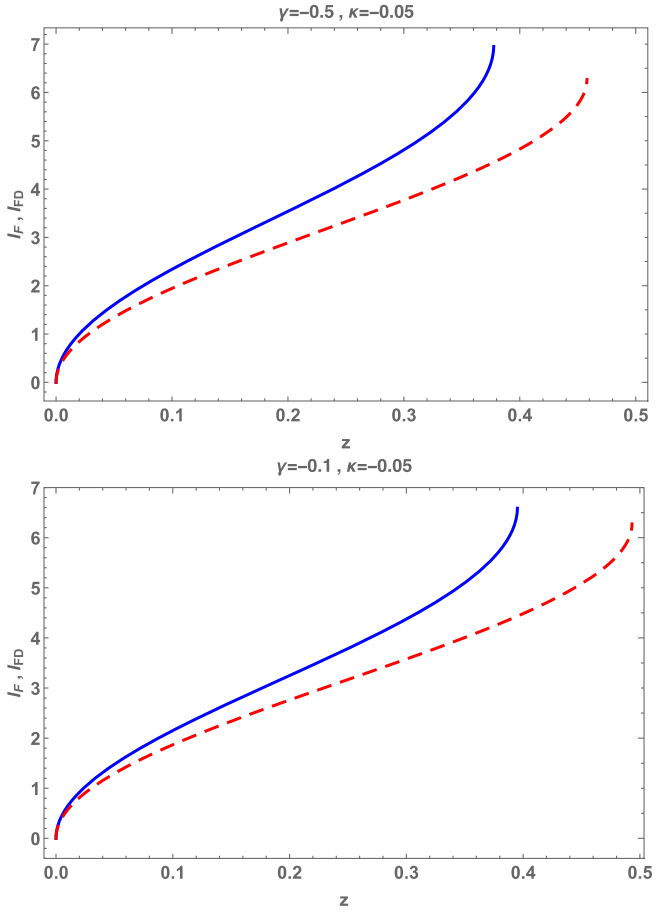

FIG. 4. The total angle integrals I_F and I_{FD}. The solid blue (in color) curve denotes the present approximation of I_{FD} by Eq. (67) and the dashed red (in color) curve denotes numerical calculations of I_F in Eq. (19), where we assume the same values for κ and γ in Fig. 3. For the simplicity, we choose $z \equiv z_R = z_S$, which is denoted by the horizontal axis. For $z \ll 1$, the two curves are very close to each other, because the quadratic approximation works well especially near $z \sim 0$. The two curves are close to each other especially for smaller z. For instance, the difference between them is roughly 20% at $z \sim 0.2$. A significant deviation at large z reflects a departure from the quadratic approximation of $H(z)$ in z.

calculations for I_{FD}. As shown in Fig. 3, f is dependent rather strongly on γ. The difference between the numerical f and an approximate one becomes significant as z is larger. On the other hand, the closest approach and its vicinity make a dominant contribution to the total angle integral I_F. In Fig. 4, therefore, I_F shows much weaker dependence on γ and z.

Finally, we discuss the gap size. By using Eq. (64) for Eq. (50), we obtain

$$\Delta b = \frac{b_m^3 z_L^2}{8 r_m^2}. \tag{70}$$

For $b_m \sim r_m$, it becomes simply

$$\Delta b \approx \frac{1}{8} b_m z_L^2. \tag{71}$$

In a SSS spacetime, the photon sphere was thought to be always an edge such as the inner boundary of a black hole shadow. However, Eqs. (70) and (71) provide a counterexample, when the PS is stable.

V. CONCLUSION

We demonstrated that the location of a stable PS in a compact object is not always an edge such as the inner boundary of a black hole shadow. We showed also that a

SSS spacetime cannot be asymptotically flat, when the SOPS exists in the spacetime.

We proved a proposition that the closest approach of a photon is prohibited in the immediate vicinity of the stable PS when the photon is emitted from a source (or reaches a receiver) distant from a lens object. We discussed the gap size. Because of the existence of the gap, the mild deflection is caused for a photon traveling around the stable PS which exists in a class of SSS spacetimes.

Finally, we used a class of SSS solutions in Weyl gravity in order to exemplify the mild deflection near the stable outer PS. It would be interesting to examine whether a light ray is mildly deflected around a stable photon surface in a less symmetric or dynamical spacetime. It is left for the future.

ACKNOWLEDGMENTS

We would like to thank Mareki Honma for the conversations on the EHT method and technology. We wish to thank Keita Takizawa, Naoki Tsukamoto, Chul-Moon Yoo, Kenichi Nakao, Tomohiro Harada, and Masaya Amo for useful discussions. We thank Yuuiti Sendouda, Ryuichi Takahashi, Masumi Kasai, Kaisei Takahashi, and Yudai Tazawa for useful conversations. This work was supported in part by Japan Society for the Promotion of Science (JSPS) Grant-in-Aid for Scientific Research, No. 20K03963 (H. A.), in part by Ministry of Education, Culture, Sports, Science, and Technology, Grant No. 17H06359 (H. A.).

[1] F. W. Dyson, A. S. Eddington, and C. Davidson, Phil. Trans. R. Soc. A **220**, 291 (1920).
[2] K. Akiyama *et al.* (Event Horizon Telescope Collaboration), Astrophys. J. **875**, L1 (2019); Astrophys. J. **875**, L2 (2019); Astrophys. J. **875**, L3 (2019); Astrophys. J. **875**, L4 (2019); Astrophys. J. **875**, L5 (2019); Astrophys. J. **875**, L6 (2019).
[3] K. Akiyama *et al.* (Event Horizon Telescope Collaboration), Astrophys. J. **910**, L12 (2021).
[4] K. Akiyama *et al.* (Event Horizon Telescope Collaboration), Astrophys. J. **910**, L13 (2021).
[5] C. Darwin, Proc. R. Soc. A **249**, 180 (1959).
[6] V. Bozza, Phys. Rev. D **66**, 103001 (2002).
[7] N. Tsukamoto, Phys. Rev. D **95**, 064035 (2017).
[8] N. Tsukamoto, Phys. Rev. D **102**, 104029 (2020).
[9] N. Tsukamoto, Phys. Rev. D **104**, 064022 (2021).
[10] N. Tsukamoto, Phys. Rev. D **104**, 124016 (2021).
[11] V. Perlick, Living Rev. Relativity **7**, 9 (2004).
[12] N. G. Sanchez, Phys. Rev. D **18**, 1030 (1978).
[13] C. M. Claudel, K. S. Virbhadra, and G. F. R. Ellis, J. Math. Phys. (N.Y.) **42**, 818 (2001).
[14] S. Hod, Phys. Lett. B **727**, 345 (2013).
[15] Y. Decanini, A. Folacci, and B. Raffaelli, Phys. Rev. D **81**, 104039 (2010).
[16] S. W. Wei, Y. X. Liu, and H. Guo, Phys. Rev. D **84**, 041501 (R) (2011).
[17] I. Z. Stefanov, S. S. Yazadjiev, and G. G. Gyulchev, Phys. Rev. Lett. **104**, 251103 (2010).
[18] M. Cvetic, G. W. Gibbons, and C. N. Pope, Phys. Rev. D **94**, 106005 (2016).
[19] G. W. Gibbons and C. M. Warnick, Phys. Lett. B **763**, 169 (2016).
[20] T. Ohgami and N. Sakai, Phys. Rev. D **91**, 124020 (2015).
[21] Y. Koga and T. Harada, Phys. Rev. D **94**, 044053 (2016).
[22] Y. Koga and T. Harada, Phys. Rev. D **98**, 024018 (2018).
[23] Y. Koga, Phys. Rev. D **99**, 064034 (2019).
[24] Y. Koga, Phys. Rev. D **101**, 104022 (2020).
[25] Y. Koga, T. Igata, and K. Nakashi, Phys. Rev. D **103**, 044003 (2021).
[26] T. Shiromizu, Y. Tomikawa, K. Izumi, and H. Yoshino, Prog. Theor. Exp. Phys. **2017**, 033E01 (2017).
[27] H. Yoshino, K. Izumi, T. Shiromizu, and Y. Tomikawa, Prog. Theor. Exp. Phys. **2017**, 063E01 (2017).
[28] H. Yoshino, K. Izumi, T. Shiromizu, and Y. Tomikawa, Prog. Theor. Exp. Phys. **2020**, 023E02 (2020).
[29] H. Yoshino, K. Izumi, T. Shiromizu, and Y. Tomikawa, Prog. Theor. Exp. Phys. **2020**, 053E01 (2020).
[30] R. Yang and H. Lu, Eur. Phys. J. C **80**, 949 (2020).
[31] K. Izumi, Y. Tomikawa, T. Shiromizu, and H. Yoshino, Prog. Theor. Exp. Phys. **2021**, 083E02 (2021).
[32] C. Cederbaum and G. J. Galloway, Classical Quantum Gravity **33**, 075006 (2016).
[33] A. K. Mishra, S. Chakraborty, and S. Sarkar, Phys. Rev. D **99**, 104080 (2019).
[34] C. Cederbaum and G. J. Galloway, J. Math. Phys. (N.Y.) **62**, 032504 (2021).
[35] M. Guo and S. Gao, Phys. Rev. D **103**, 104031 (2021).
[36] R. A. Konoplya and A. Zhidenko, Phys. Rev. D **103**, 104033 (2021).
[37] Q. Gan, P. Wang, H. Wu, and H. Yang, Phys. Rev. D **104**, 024003 (2021).
[38] R. Ghosh and S. Sarkar, Phys. Rev. D **104**, 044019 (2021).
[39] M. Siino, Classical Quantum Gravity **38**, 025005 (2021).
[40] M. Siino, ArXiv:2107.06551.
[41] K. Takizawa and H. Asada, Phys. Rev. D **103**, 104039 (2021).
[42] V. Bozza, Phys. Rev. D **78**, 103005 (2008).
[43] K. Takizawa, T. Ono, and H. Asada, Phys. Rev. D **101**, 104032 (2020).
[44] K. Takizawa, T. Ono, and H. Asada, Phys. Rev. D **102**, 064060 (2020).
[45] P. V. P. Cunha, E. Berti, and C. A. R. Herdeiro, Phys. Rev. Lett. **119**, 251102 (2017).
[46] S. Hod, Phys. Lett. B **776**, 1 (2018).
[47] W. Hasse and V. Perlick, Gen. Relativ. Gravit. **34**, 415 (2002).

[48] A. Ishihara, Y. Suzuki, T. Ono, T. Kitamura, and H. Asada, Phys. Rev. D **94**, 084015 (2016).
[49] A. Ishihara, Y. Suzuki, T. Ono, and H. Asada, Phys. Rev. D **95**, 044017 (2017).
[50] T. Ono, A. Ishihara, and H. Asada, Phys. Rev. D **96**, 104037 (2017).
[51] T. Ono and H. Asada, Universe **5**, 218 (2019).
[52] V. Cardoso, L. C. B. Crispino, C. F. B. Macedo, H. Okawa, and P. Pani, Phys. Rev. D **90**, 044069 (2014).
[53] J. Keir, Classical Quantum Gravity **33**, 135009 (2016).
[54] A. Addazi, A. Marciano, and N. Yunes, Eur. Phys. J. C **80**, 36 (2020).
[55] T. Chiba and M. Kimura, Prog. Theor. Exp. Phys. **4**, 043E01 (2017).
[56] There is a prohibited region around the stable PS as shown in Sec. III D. Because the existence of this gap region, the functions H and f are not differentiable at $r = r_m$. As a result, H and f cannot be Taylor-expanded around r_m. In stead of Taylor expansions, therefore, we look for asymptotic expansions of I_F, I_{FD} and I_{FR} through f, f_D and f_R.
[57] P. D. Mannheim and D. Kazanas, Astrophys. J. **342**, 635 (1989).
[58] G. E. Turner and K. Horne, Classical Quantum Gravity **37**, 095012 (2020).
[59] Turner and Horne realized that a bound orbit of a photon is possible in this parameter region for the SSS solution in Weyl gravity [58].